Interaction with virtual aesthetic shapes through a desktop mechatronic system

Mario Covarrubias* and Monica Bordegoni

KAEMaRT Group, Department of Mechanical Engineering, Politecnico di Milano, Milano, Italy

(*Received 2 July 2013; accepted 3 October 2013*)

1. Introduction

The Desktop Mechatronic System (DMS) that is presented in this paper allows a continuous and smooth free hand contact interaction on a real and developable physical strip actuated by a servo-controlled mechanism. The objective of the system is to add to the visual rendering of a surface a consistent physical rendering of selected cross-sectional curves. This intends to be a tool supporting industrial designers during the creation, evaluation and modification of the design of the shape of new products. During the development of new concepts, designers need to physically interact with the evolving shape of the product they are designing so as to check and evaluate its aesthetic features. This is typically done by using physical prototypes built with traditional production processes. Rapid prototyping techniques are also valuable for this purpose. Actually, 'rapid' should be interpreted in terms of hours or even days, and besides, a rapid prototype can be used solely as a display, and not as a full interface for both input and output handling of the shapes. However, in the DMS the handling of the shapes occurs in only one direction and is used as an output display. Although physical prototypes are a good means for product evaluation, they also add some limitations; for example, they do not allow variants of shape and material, and they do not support easy shape modification and immediate correlation with the corresponding digital model. In addition, the production of the physical prototype is costly and time consuming, especially with respect to the other product design phases.

A physical prototype is typically built after performing a detailed design and functional analysis of the product and of its components. So, typically a design engineer works with two or more software tools for performing modelling and analysis, in

*Corresponding author. Email: mario.covarrubias@polimi.it

order to check that all the design constrains are satisfied. There are several commercial Computer Aided Design (CAD) and analysis tools that are widely used in the design industry for this purpose. Currently, a CAD tool provides a geometric model in standard formats such as STL, STEP or IGES, which can be used as input to a Computer Aided Engineering (CAE) and/or to an analysis tool. Typical problems related to the file exchange are the loss of information (Cao *et al*. 2009) and breakdown of the parametric properties of the CAD model.

This research proposes a methodology using CAD and associativity properties to maintain the parametric features of the three-dimensional (3D) model of the design shape. We propose to integrate the CAD and multi-body associativity with the Desktop Mechatronic System allowing simultaneous visual and haptic interaction with the shape model. This new haptic interaction modality, combined with traditional visualisation, aims to allow designers to evaluate new shapes through the sense of touch in addition to vision. In this way, the manual skills and sensitivity of designers can be exploited by offering them an operating modality which is very close to their habits and usual way of working.

The DMS consists of a servo-actuated strip that physically renders cross-sectional curves of a surface. The strip is represented using a Minimal Energy Curve (MEC) spline approach, where a developable surface is rendered taking into account the CAD geometry of the virtual shapes. In this way, the design process can also be controlled according to well-defined engineering concepts and drawings taking advantage of the parametric constraints and technical dimensions.

The paper is organised as follows. Section 2 presents an overview of related works. Section 3 shows the basic concept of the Desktop Mechatronic System. In Section 4 we present the transmission system. Section 5 describes the real prototype and its limits. Section 6 describes the integration and associativity approach. In Section 7 the positioning system that implements the DMS is described. Section 8 presents the results of the studies about the validation of the accuracy of the system and finally, Section 9 draws some conclusions.

2. Related works

Interaction with object surfaces is one of the most common experiences for people in everyday life, which happens through tactile and proprioceptive (haptic) senses. Several visual displays of object surfaces rely on illusions created for the eyes, essentially fooling the mind into interpreting a flat screen as a 3D image. In order to improve the surface perception, the visual interpretation of the surface features is reinforced with haptic experience as reported in Menelas *et al*. (2008)

Regarding the specific problem of physically representing shapes, several research works in the field of haptics have addressed the problem of representing correctly curves and curvature information, overcoming the limits of point-based devices, and providing cutaneous information to the fingers. In Dostmohamed and Hayward (2005) an attempt to give the illusion of touching a haptic shape solely through the communication of the local tangency of the curve on one or more fingertips is presented. This device does not provide enough kinesthetic cues, especially for large curves. Frisoli *et al*. (2008) describe a haptic device that is the combination of a point-based device providing kinesthetic cues, and a fingertip haptic device providing cutaneous cues. In Provancher *et al*. (2005) an attempt to communicate curves and curvature information through a contact location feedback on the fingertips is described.

The main limitation of these research works is that users interact with the shape using only a part of the hand, mainly one or a couple of fingers, and not with the whole hand. In the application domain of product design that we address, the possibility of touching and exploring a surface with the whole hand is of primary importance. In this regard, some research activities have addressed the limits of human perception and discrimination of curvature in a whole-hand exploration like those reported in Pont *et al*. (1997), and Sanders and Kappers (2009). These studies are of great utility in the development of new full-hand haptic devices because they provide several guidelines, on the basis of haptic curve discrimination and haptic shape perception.

Several research works in the field of mechatronics and control have presented interesting control metaphors. For example in Senkal and Gurocak (2011), a new 2 degrees of freedom (DOF) hybrid actuator concept is explored as a powerful and compact alternative to conventional haptic actuators; Giberti *et al*. (in press) present the design of a five-bar parallel manipulator with 2-DOF highlighting the multi-disciplinary approach used in its development, and Gonenc and Gurocak (2012) present the control scheme which determines the motor and brake inputs separately based on their capabilities. However, these works do not investigate the control metaphor where the actuators are directly driven by the 3D model as needed in our system.

The problems of computer-controlled shaping, even in real-time, of a strip made of metallic material were addressed by several researchers in the past, who focused on a kind of free shaping of a heated cutting blade for free form cutting of rigid plastic foam slabs for layered object manufacturing (Horváth *et al*. 1998a, 1998b, Broek *et al*. 2004). These researchers have developed the mathematical/technological fundamentals and process of free-form cutting based on heated flexible blades. The shape and the relative positions of the flexible blade are controlled continuously as needed by the normal curvatures of the front faces of the layers. They based their computation on the Kallay-algorithm (Kallay 1987), but did not manage to reduce the elapsed computational time below a threshold which is acceptable for direct free hand interaction.

The haptic strip we have studied, which is described in this paper, is an attempt to develop a haptic system that tries to

reproduce exactly the shape of a mathematical curve, by deforming a physical continuous strip, in order to give users the possibility to have a full-hand contact with the virtual surface. The system is able to communicate both tactile and kinesthetic cues through a full-hand interaction.

In our research group we have been developing haptic devices to permit touch interactions between human users and virtual objects. All the previous mechatronic devices related to the haptic strip have been developed on the context of the SATIN project (Bordegoni *et al*. 2010). This haptic interface, described in detail in our previous work, consists of a flexible strip that is held in space in front of the users by two HapticMaster systems (Lammertse *et al*. 2002). The first version of the haptic strip (Bordegoni *et al*. 2009a) has been developed with the main objective of just integrating the various mechanical components in order to validate the concept at the basis of the strip, which is related to the cutting plane metaphor. Subsequently, a higher performing version of the haptic strip (Bordegoni *et al*. 2009b, Bordegoni *et al*. 2011) has been designed, with the aim of extending the domain of curves that can be haptically rendered; the second strip is capable of rendering geodesic trajectories in addition to planar ones. The mechanical configuration of both versions of the strip achieves a minimum bending radius of 180 mm, which directly limits the domain of curves that the haptic strip is able to represent. Obviously, the smaller the bending radius of the haptic strip, the larger the domain of virtual shapes that is possible to render. In both configurations of the haptic strip (planar and geodesic), the device is able to reproduce curves that lie on the virtual object. The SATIN haptic system set-up in its entirety is not portable, and is also expensive due to the cost of the set of components constituting the strip.

The main idea in the design and development of the Desktop Mechatronic System (DMS) described in this paper consists of adopting the concept developed in the previous haptic system, which proved to be good for the target applications, and introducing some improvements. First, the new DMS system is of desktop type, and therefore lighter and portable. In addition, it improves the minimum bending radius, by reaching 30 mm when representing a concave shape, and 20 mm when representing a convex shape.

A first attempt to replicate the concept proposed in the SATIN project has been explained in Covarrubias *et al*. (2013) by using the non-equidistant interpolation points technique. Actually, this solution has a limit when representing concave profiles, because the control joints of the strip can be too close, thus decreasing the precision of the shape rendering.

3. The concept

The mechatronic device presented in this paper consists of a servo-actuated developable metallic strip physically representing geometric curves laying on the surface of a 3D model. The haptic interaction occurs through a 2D cross-section curve of the virtual object surface, which is obtained by intersecting the virtual 3D object with a virtual cutting plane. The basic concept is to use the virtual cutting plane as an interaction tool with the virtual object. The 2D cross-section to render physically can be selected by just moving the cutting plane. Figure 1-a shows an example of a 2D cross-section curve of a virtual vacuum cleaner. Figure 1-b shows the real vacuum cleaner and a tape attached on its surface, which is a practice typically used by designers in the conceptual phase of a new product design for highlighting style curves. The approach based on the 2D cross-section curve of the virtual object surface intends to mimic this practice. A portion of this 2D cross-section corresponds to the target curve on which the strip has to be located. The physical strip, represented by the blue curve in Figure 1-c, is initially in its nominal position and is defined by a set of equidistant elements. Then the strip is bent as a Minimal Energy Curve (MEC) spline, and the spline interpolation points are positioned in the same place as the joints of the equidistant elements.

3.1 Equidistant interpolation points and equilibrium of forces

This section describes the approach used to approximate the physical strip to the 2D cross-section curve. The strip is represented by six interconnected elements of the same length. The seven extremities of the segments are the interpolation points. A multi-body model of the kinematic device actuating the deformation of the strip is used for studying the strip bending. The main frame on which the interpolation points rely is a chain consisting of alternating rigid struts and pivots with torsion springs. Such a chain, with spring torque indicated schematically at each pivot point, is shown in Figure 2. The multi-body analysis has considered both the number and lengths of the elements required by the physical structure.

When an elastic strip is in a minimal energy configuration, it is in mechanical equilibrium. This means that the sum of force values on a point along its length is zero. Each element generates a tension force at the extremities, in the same direction as the element length (indicated by 'T'). At each pivot there is a spring generating force tending to straighten out the chain, i.e. towards a turning angle of zero. The turning angle is denoted by ϕ and the force generated by the moment (or spring torque) by M. At the endpoints, the force generated by the moment is normal to the strut joining the centre to the endpoint. According to Newton's third law, the sum of all forces arising from the element must be zero, so there is a balancing force at the centre point equal to the vector sum of the force values at the endpoints, pointing in the opposite direction. In the simulation performed in the multi-body analysis, we assume that the spring at the pivot point is purely elastic, which means that the moment (torque) is proportional to the turning angle as can be seen in Figure 2. The moment

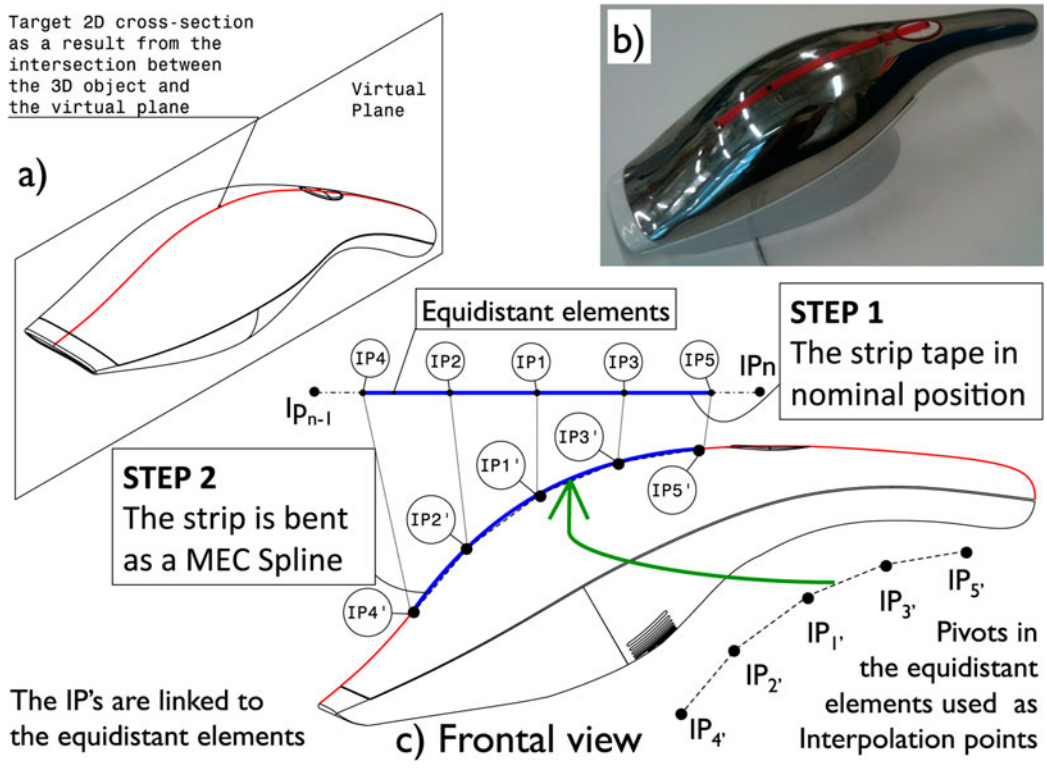

Figure 1. MEC spline approach for representing the 2D cross-section curve.

(torque) on each pivot point is represented by the torsional springs that are located at the points IP1, IP2, IP3, IP4, and IP5.

When these elements are linked together in a chain, there are five force vectors acting on a single pivot point: the tension force from each adjoining element TE2 and TE4; the moment forces from the previous and next pivots in the chain (ME2 and ME4), and the balancing force 2MCos($\Delta\phi$/2). Note that the pivots of the elements are used to assign two constraints to the spline. Each constraint can rotate freely. Besides, it can allow the spline to slide freely as can be seen from the detailed view in figure. In the equidistant main frame the number of elements (E) and the distance between them (A) have been considered. The results of the multi-body analysis are presented in the next section.

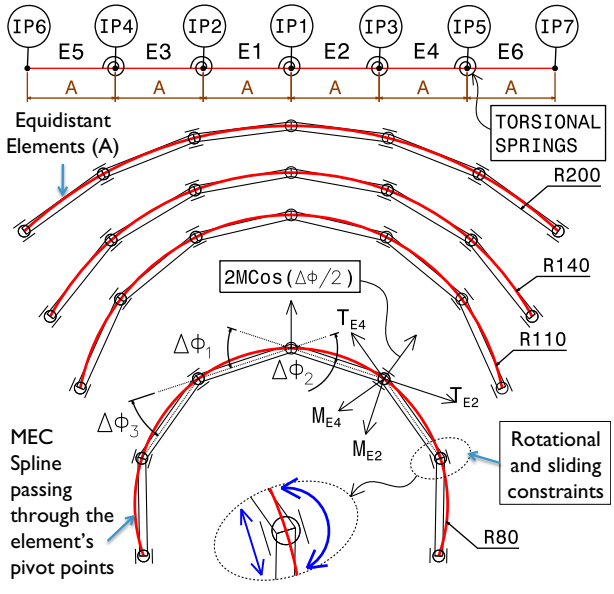

Figure 2. Forces on a single pivot point in a chain.

3.2 The minimal energy curve (MEC) spline interpolation approach

In order to better approximate the virtual 2D cross-section with the real metallic strip, we decided to use the Minimal Energy Curve (MEC) spline approach. This approach simplifies the conformation of the metallic strip on the virtual shape. In practice, the physical strip is able to approximate the shape of the virtual object surface by adopting the shape of a MEC spline, i.e. the strip can only morph itself into a twice continuously differentiable function constructed of piecewise third-order polynomials, which pass through a set of several equidistant interpolation points. The main idea behind the MEC spline is based on the designer's tool used to draw several and smooth curves crossing a number of points. This spline consists of interpolation points attached to a flat element at the endpoints. Our mechatronic device, in fact assumes this

approach in which the flexible stripe is bent across each of these interpolation points, resulting in a pleasingly smooth curve. The interpolation points are numerical data driven by its position and orientation on the virtual model. In fact, these data are used in order to control the actuators. These interpolation points 'bend' the strip so that it passes through each of the interpolation points without any erratic behaviour or break in continuity. Note that the quality and precision of the MEC spline depends on both the number and the distance between the interpolation points.

4. Transmission system

A Modal Frequency Response analysis has been performed in order to simulate the bending process according to the mechanical properties of the metallic strip. This Modal Frequency Response analysis includes several materials such as for example aluminium, steel and copper. In addition, we decided to modify the thickness of the strip, by using three values: 1 mm, 2 mm and 5 mm.

Then, the results of the analysis are used in the ADAMS-Flex tool, in order to obtain the force values required to bend the strip as a flexible element rather than as a rigid body element. These values have been used to select the actuators. In fact, the servo drives have been selected so as to guarantee high reliability; the servo motor with titanium gears provides up to 2.35 Nm of continuous torque. The servo drives are HS-5955TG manufactured by HITEC (Hitec 2012). This allows us to get high stiffness and load capacity.

The length of the strip and the distance from each interpolation point have been assigned taking into account the servo motor size and the collision constraints assigned on the motion simulation performed with the multi-body analysis tool. The total length of the metallic strip is 270 mm, and it has been divided in six segments with seven interpolation points. Each segment is 45 mm long. This means that the haptic strip can display curves with a maximum length of 270 mm. This limits the kind of objects, or limits the exploration to a portion of the object surface, which the designer can feel with his fingers or hand. This issue has been considered and a solution based on a positioning system has been proposed for increasing the working volume, which is described in Section 7.

4.1 Combined transmission system

Combining the absolute with relative actuation requires a unique virtual interaction model. This is needed because, as can be seen in Figure 3, the central motors are used as absolute actuators while the motors located on their extremities are used as relative actuators.

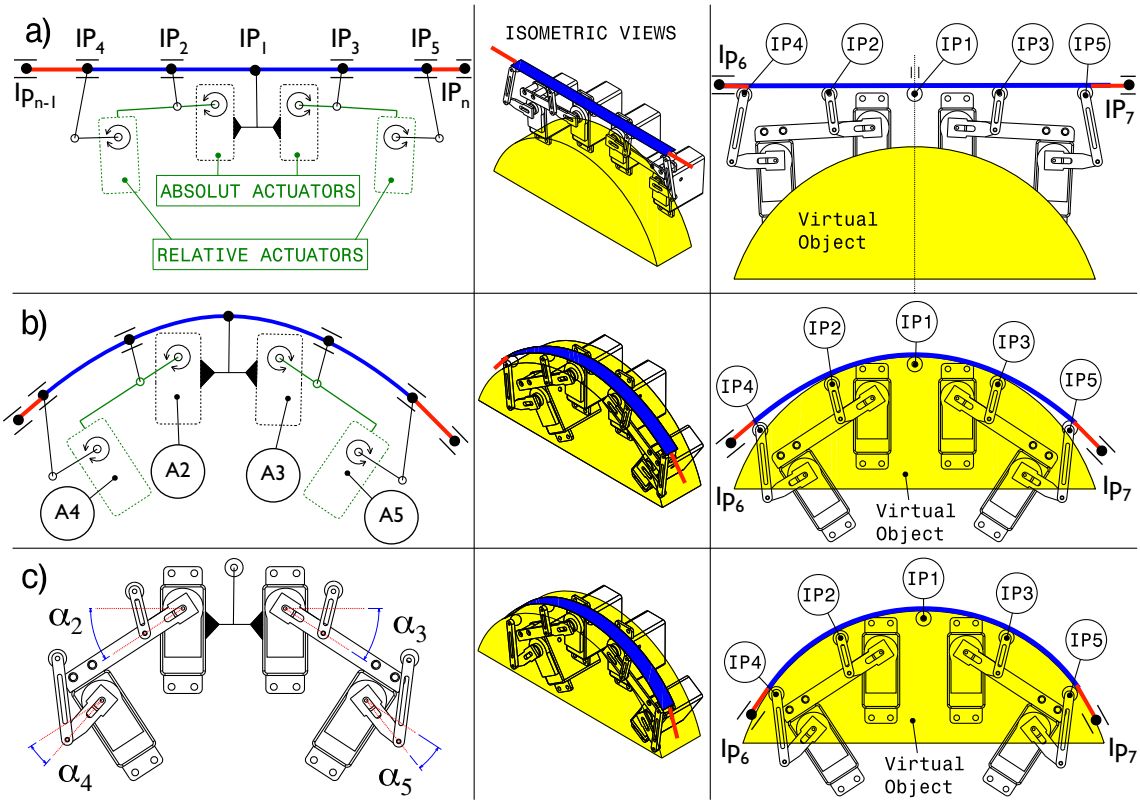

Figure 3. Mechanism used to actuate the mechatronic device.

The position of the interpolation points changes on the basis of the geometry of the virtual object. The interpolation points are required to be positioned correctly while in contact with the virtual surface. The algorithm that drives this continual computation of contact location is based on the control of the seven interpolation points using the Minimal Energy Curve Spline approach.

For each single interpolation point an αs angle is required, the αs1 angle required by the servo motor is exactly the same α1 angle computed while the strip takes the shape of the virtual object. We decided to include bending moments through side forces on each module by using single push rods.

The mechatronic device requires the combination of seven interpolation points to reproduce both convex or concave surfaces, and a combination of those. The shapes that can be represented exactly with the developable strip driven by side force actuators have been analysed. The first column on Figure 3-a shows the instant in which a cylindrical surface is reached. Note the kinematic diagram in which are used the absolute and relative approaches on the servo actuators array.

The servo motors A2 and A3 (Absolute actuators) are clamped to Interpolation Point 1 (IP1). IP1 is linked through a rigid joint on slot constraint with the virtual environment. This constraint guarantees the sliding motion on the 'Z' axis. The servo motor A2 is responsible for changing the position and orientation of Point 2 (IP2). The servo motor A3 is responsible for changing the position and orientation of Point 3 (IP3), and so on. Note that servo motor A4 is relatively linked to servo motor A2 and in the same way, servo motor A5 is relatively linked to servo motor A3.

5. Real prototype and its limits

A real prototype of the system based on the studies previously described has been manufactured taking into account some important considerations related to the use of sheet metal components that implies: low inertia, light weight parts and low friction. For the haptic strip a critical concern is the component stiffness while reaching the target surface. In order to provide this stiffness, the links have been designed as beams or shell structures. This solution provides a lighter and rigid module for bending. Furthermore a finite element method (FEM) analysis was carried out in order to verify both the displacements and stress in the critical components of the strip mechanism. In addition, the mounting arrangement of the set of actuators housing has been designed to accommodate manufacturing tolerances. Figure 4-a shows the frontal view of the prototype of the desktop mechatronic device with the absolute and relative actuators.

Figure 4-b shows the top view, in which the metallic strip is located on the seven interpolation points. This configuration has been considered in order to prevent collisions between the components. Figure 4-c shows the desktop-mechatronic prototype in which the combination of the transmission system

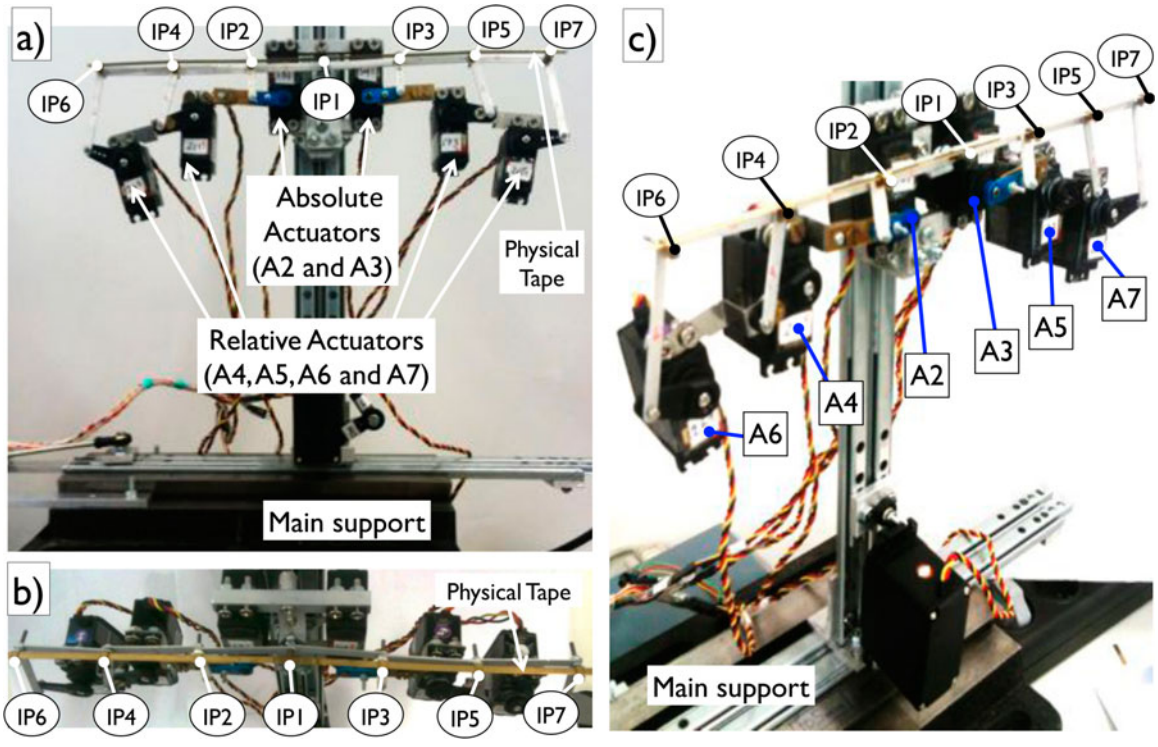

Figure 4. Prototype of the mechatronic device.

has been used and the interface linked to the multi-body analysis tool.

5.1 Limits of strip bending

Figure 5 shows different instants of the physical rendering process in which the system displays a combination of convex and concave shapes without having any collision between the servo actuators and the mechanical components.

As can be seen, the minimum bending radius is 30 mm when representing a concave shape, and 20 mm when representing a convex shape.

5.2 Damping shock absorption system

This section presents the implementation of a plastic collision in the simulation, which eventually is used to compute the necessary angles which are used as a reference for the motors. The damping shock absorption system has been modelled with a stiff linear spring in parallel with a linear damper in order to dissipate the kinetic energy of the objects when colliding. Seven virtual springs/dampers have been added as can be seen in Figure 6. Each interpolation point is linked to a virtual spring, i.e. IP1 is linked to the ground through VS1, then IP2 is linked to the servomotor frame through the lever, and so on. The positions of the springs and their effects have been considered in order to always have a pre-load in the servo-actuators. The multi-body system allows us to change the governing equations of constraints and thereby to create any desired spring/damper combination.

It is also possible to incorporate logical tests into the analysis, and apply different equations under different conditions. The seven virtual springs are modelled as a damping shock absorption system with the following values:

$$Spring\ Force = -kx \tag{1}$$

$$Damper\ Force = -cv \tag{2}$$

- Spring natural length = 25 mm
- k = 0.2 N/mm
- c = 0.004 Ns/mm

The results shown in Figure 6 are typical for a mildly under damped system that oscillates several times before coming to rest.

6. Associativity for design tools integration

In the process of creating new shapes, designers often need to touch the surfaces of their products, in order to check and evaluate their aesthetic quality. This practice allows them to better evaluate the shapes in terms of geometric properties. Typically designers use Computer Aided Design (CAD) tools to create new shapes, exploiting the feature-based and parametric approaches. The novel haptic system that we propose for the evaluation of the designed digital shapes uses the MSC visualNastran 4D tool (VN4D) to control the mechatronic

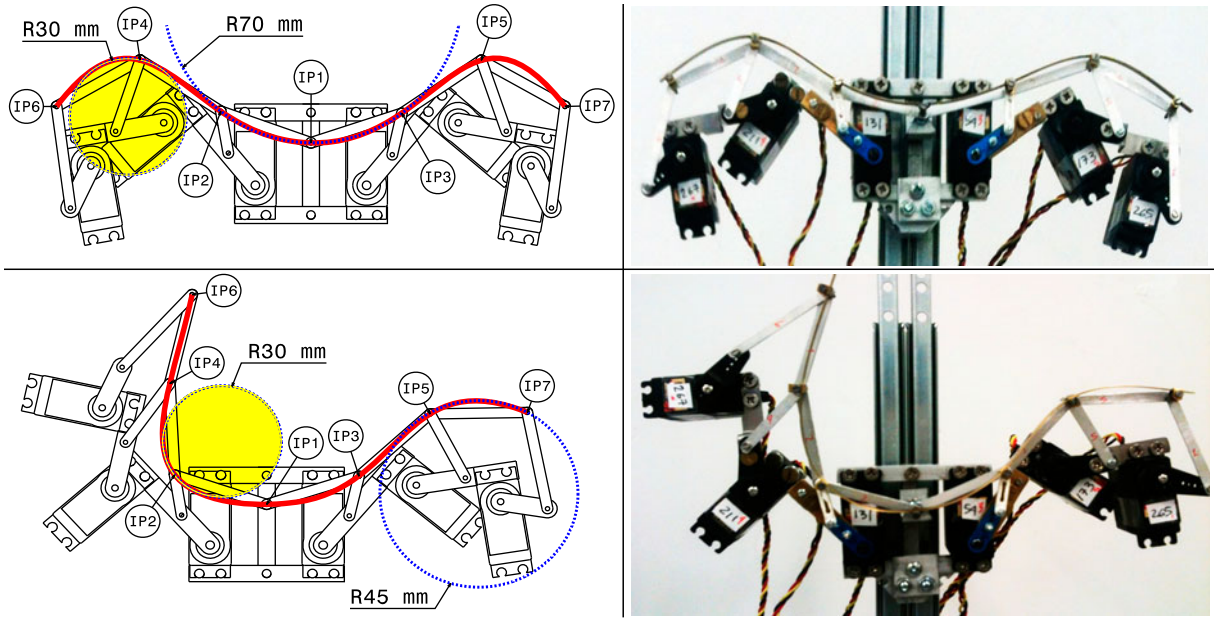

Figure 5. Limits in radius curvature.

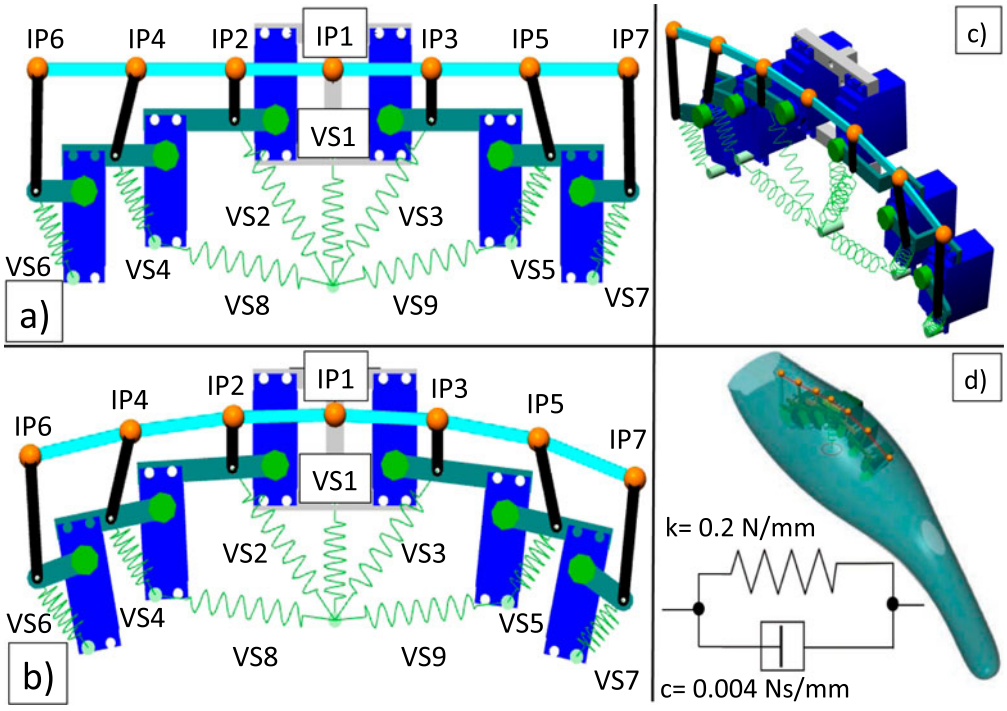

Figure 6. Virtual springs-dampers array.

system and physically render the selected curve. In order to do that, the CAD model of the object has to be converted into a VN4D model, and a relation between the two models must be preserved, in order to allow consistent modifications of the geometry.

Therefore, we have defined a framework supporting an efficient approach based on a set of tools including a CAD tool, and multi-body and Mathworks Matlab/Simulink applications. The CAD tool is used to create and manage the geometry of the object, multi-body and Mathworks tools are used to offer extensive libraries of existing dynamic elements for modelling constraints, which allow users to construct complex constraint equations and to input complex forcing functions.

Figure 7 shows the conceptual scheme of our approach. On the left hand side the 3D model is represented; the user models the 3D object by means of any commercial CAD tool (for example, Autodesk Inventor, Pro/Engineer, Siemens Solid Edge, DS SolidWorks etc.), then the model is directly imported into the multi-body environment.

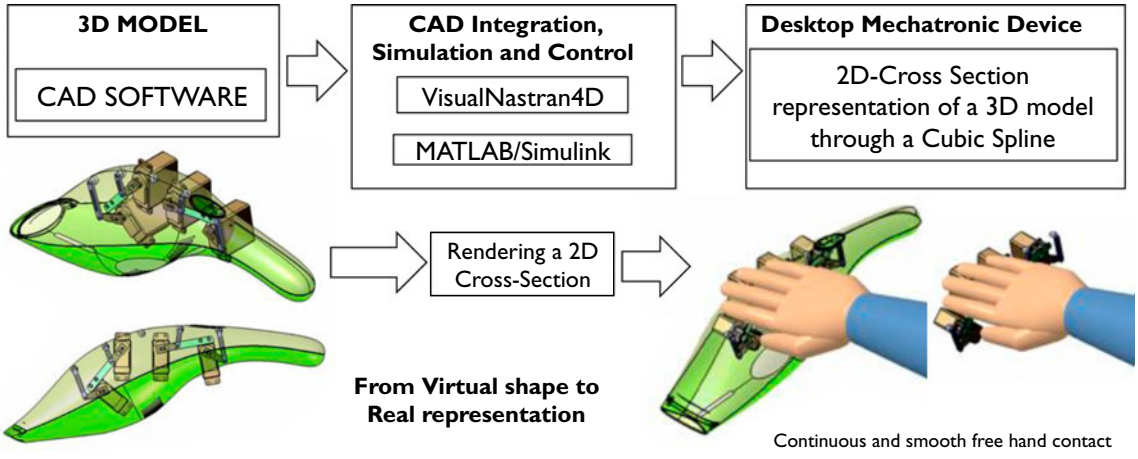

Figure 7. Integration of the tools and associativity.

The central column in Figure 7 shows the CAD integration and associativity properties, where the dynamic modelling with VN4D is extended to include control with the integration of Simulink. VN4D is used to construct the dynamic model, while Simulink is used to design the control system. A VN4D library is inserted as a block (vNPlant) into the Simulink model, allowing feedback between the control system and the dynamic model.

Finally, the column on the right hand side shows the integration with the desktop mechatronic device, which reproduces a 2D cross-section of a 3D surface model. These relationships preserve the identities of the CAD components and the corresponding imported components of the VN4D simulation environment. The VN4D exporter function defines these unique identities from the CAD assembly component, and embeds them in the exported model (i.e. in STEP, STL or IGES file formats).

However, this associativity is not completely symmetrical between the CAD and the multi-body tool, because the translation process occurs in only one direction, from the CAD environment to the generated VN4D model. Therefore, if the designer wishes to modify some data in the main model (for example a parametric distance), he can update the CAD model, and an existing VN4D model can be used, which has been previously translated from the same CAD model. The updates do not disturb the existence and identity of the VN4D model components corresponding to the original CAD assembly components.

6.1 CAD, multi-body associativity and DMS interaction

The link between the CAD tool and the VN4D tool allows us to maintain the parametric constraints assigned by the user in the generation of the 3D model and of the technical drawing. If a modification of the geometry is required, the user is able to perform the change using the CAD tool, and this change is automatically incorporated into the VN4D simulation environment. Through a technical drawing of an object, several dimensions can be modified and the effect of these modifications can be physically rendered by the DMS.

As an example, Figure 8-a shows the original 140 mm distance that controls the position of one of the control points in the spline path. Obviously, the result is reached once the user presses the regeneration model option link that is located in the drawing environment. Each modification takes only a couple of seconds for the updating process, which propagates from the CAD model to the multi-body environment. Then, through the Matlab and Simulink tools, the 2D section

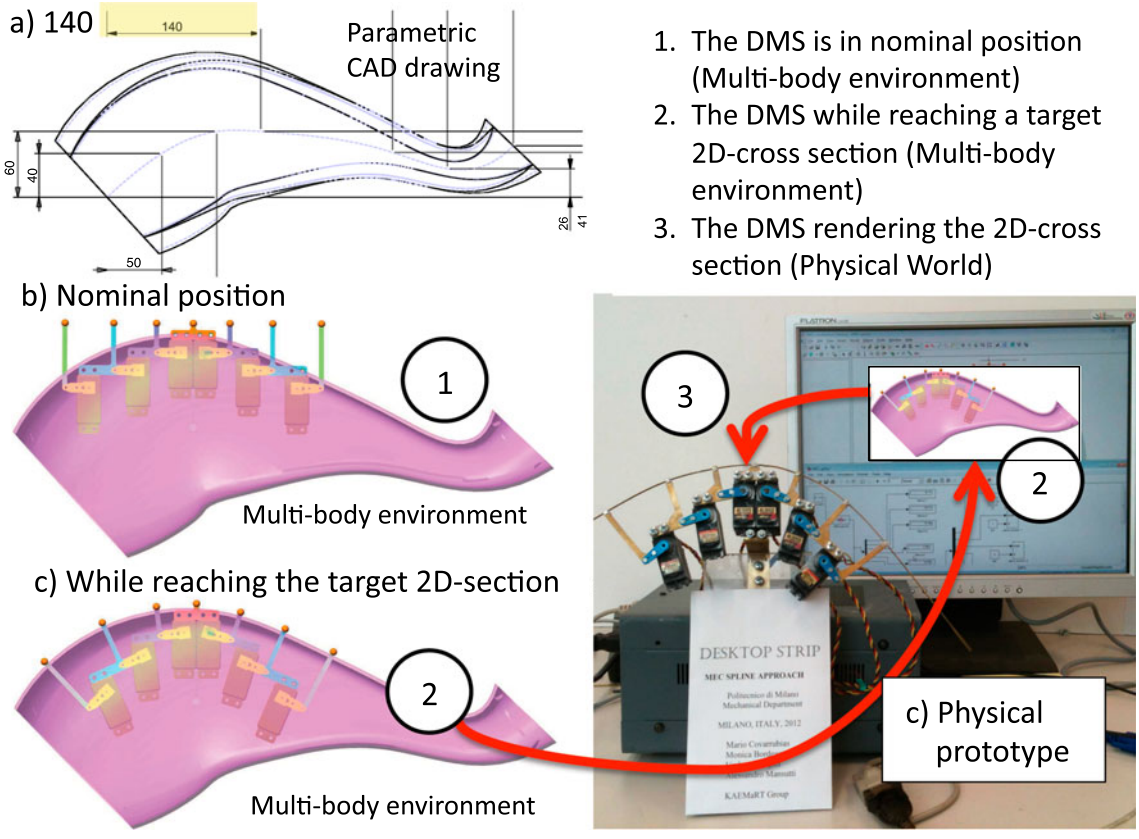

Figure 8. Modification of a technical drawing and the effect in the multi-body environment.

rendering process starts, and the DMS physically takes the shape of the virtual object.

The multi-body environment is coupled with the Mathworks Matlab/Simulink package, which merges two powerful tools into one system combining multi-body dynamics and control. As can be seen in Figure 8-b, the Desktop Mechatronic System (DMS) is in its nominal position, i.e. each of the servo-actuators angular values is null. This value guarantees the flat position of the real strip through the control of the seven interpolation points. Once the user runs the simulation, the seven interpolation points move on the virtual shape (Figure 8-c), and at the same time the DMS renders the real 2D cross-section, as can be seen in Figure 8-d. Now the user is able to feel with the palm of the hand the real 2D cross-section in order to evaluate the quality of the shape.

7. Positioning system and interaction modalities

The interaction modality offered by the Desktop Mechatronic System (DMS) permits the inspection and exploration of the virtual object by touching the physical strip. In addition, the modification of the shape of the virtual object can be performed through the CAD tool. According to the user's needs, the DMS is moved onto the virtual shape through the positioning system, which includes a physical 3-DOF platform and two virtual platforms, which are linked to the DMS and to the 3D model.

The workspace of the positioning system includes consideration of regions of limited accessibility where the physical 3-DOF platform itself may experience movement limitations. These constraints arise from limited joint travel, the link lengths, the angles between axes, or a combination of these. Additional degrees of freedom provided through the virtual platforms have been considered for increasing the working volume, which is limited by the physical 3-DOF platform, and are activated according to the interaction modality selected by the user.

The Desktop Mechatronic System provides the following interaction modalities:

(1) Positioning modality in which the user moves the DMS through the physical 3- DOF platform in order to achieve correct positioning and orienting of the strip on the virtual 3D object;
(2) Positioning modality in which the user moves the virtual object or the DMS through the virtual platform in order to enlarge the working volume that is limited by the physical 3-DOF platform;
(3) Exploration modality in which the user 'touches' the virtual 3D object in order to evaluate its shape;
(4) Modification modality in which the user modifies the 3D object by means of the parametric features of the CAD and multi-body tools. Once the modifications have been performed, the DMS is able to render the new shape.

This means that there is bi-directional interaction between the virtual and physical models, as described in Gibson *et al.* (2005), Anderl *et al.* (2006) and Liu *et al.* (2013).

7.0.1 3-DOF platform limits through L1, L2 and R1

While the workspace of the DMS attached to the 3-DOF platform defines the position and orientation that it can achieve to accomplish a task motion, the working envelope also includes the volume of the space that the DMS occupies while moving for rendering a 2D cross-section.

We decided to use the physical 3-DOF platform in a configuration as shown in Figure 9. The user interaction is performed by the positioning system through several sliders depending on the interaction modality selected.

The DMS is fixed on the 3-DOF platform through Link 1, which is actuated by servo-motor 8 (A8) providing the rotation R1 around the 'Y' axis. The dimension of this link allows the concentricity constraint between the axis of Interpolation Point 1 (IP1) and the axis of the A8 servo-actuator. In this way, the 3-DOF platform provides three real degrees of freedom through two linear guides and one rotational constraint, which are driven by three servo-actuators. L1 is driven by the user through a slider, and the actuator A0 is responsible for moving the platform on the 'X' axis. The L1 travel limit allows a 100 mm of travel motion. L2 moves the platform on the 'Z' axis through the actuator A1 and, differently from L1, this movement is not driven by the user. The servo A1 is driven from the position of interpolation point 1 (IP1) that is always moving on the virtual object. Also, this degree of freedom along the 'Z' axis provides a 100 mm of travel motion. Finally, the rotation R1 is performed through Actuator 8 (A8) providing ± 90 degrees, and its orientation value is driven by the CAD geometry.

Figure 10-a shows an instant of the simulation in which the DMS is in the nominal position that is completely flat. Then, Figure 10-b shows the instant in which all the interpolation points have been projected on the virtual shape allowing the strip to render the 2D cross-section. Note that, without the rotation R1, the DMS does not reach correctly the virtual shape due to the collisions between the actuators. In fact, as can be seen from Figure 10-c, the rotation R1 allows the entire mechanism of the strip to pivot on interpolation point 1 (IP1) allowing the strip to render the 2D cross-section without any collisions in the actuators. Figures 10-d and 10-e show additional instants of the simulation where the user moves the physical platform on the 'X' axis through actuator 0 (A0). Figure 10-f shows actuator 8 (A8), which controls R1.

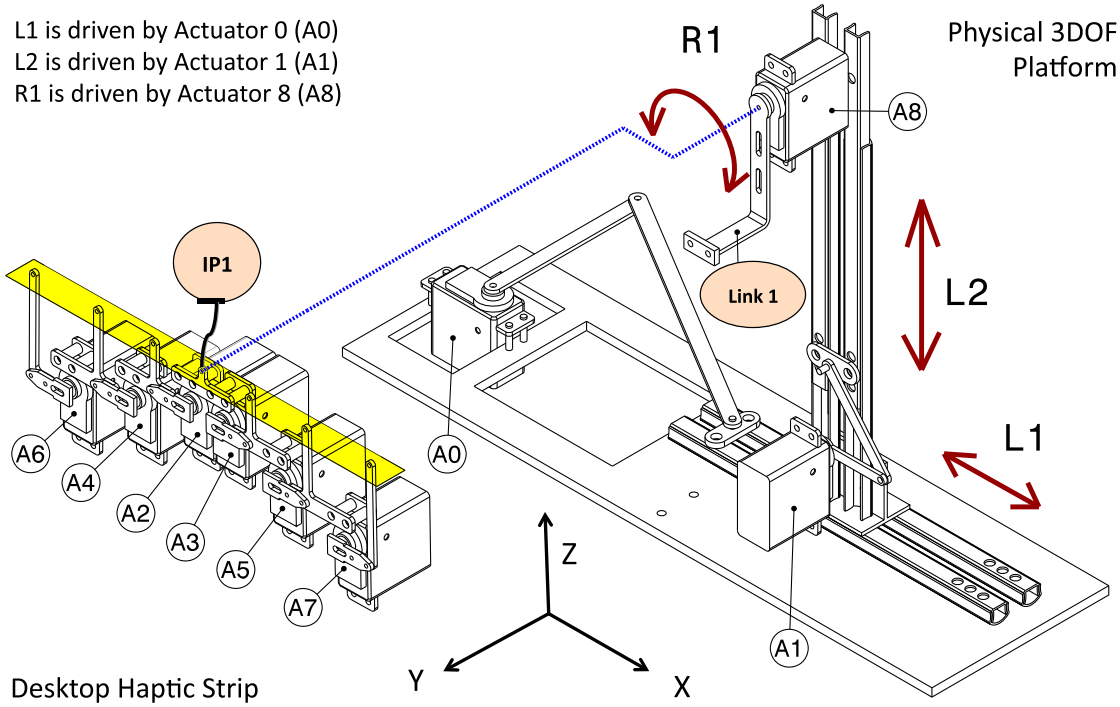

Figure 9. Physical 3-DOF platform and the DMS.

7.1 Virtual platforms

When the second interaction modality is enabled (through the virtual platforms), the DMS remains linked to the ground through a revolute slide on slot constraint. This means that the DMS can translate only along the vertical axis, and rotate around the 'Y' axis according to the IP1 position and orientation while moving on the 3D model surface, and at the same time rendering its shape through the seven interpolation points (IP1, IP2, IP3, IP4, IP5, IP6, and IP7). As can be seen in Figure 11, the user is able to move the DMS or the 3D model by using the virtual platforms that are linked to them. Through the sliders VL1, VL2 and VR1 the user is able to move the DMS, and he can also move the 3D model by using the OV1, OV2, OR1 and OR2 sliders.

In this way, the user has the possibility to locate the DMS or the 3D model, and consequently he is able to perform the evaluation of the real shape.

7.1.1 Limits on VL1

The VL1 slider that controls its linear motion is driven by the user when the 3D model remains fixed to the ground (first interaction modality described in Section 7).

Figure 12-a shows an instant of the simulation in which the DMS is moving in the VL1 direction (along 'X' axis). At this stage of the simulation, the DMS renders at the same time the 2D cross-section of the 3D Model.

Figure 12-b shows the instant of the simulation in which the DMS renders a convex shape of the 3D model. Figure 12-c shows the rendering 2D cross-section process in real time provided by the DMS, while Figure 12-d shows the user's hand while exploring the real 2D cross-section. In this case, the limits on the travel motion of VL1 and VL2 are related to the 3D object dimensions. For example, if there is a 500 x 250 x 100 mm 3D object, the travel limits on the virtual platform are 500 mm and 250 mm for VL1 and VL2 respectively. The graphics included in Figure 12 display the 'X' and 'Z' displacements of Interpolation Point 1, while moving on the 3D object.

7.1.2 Limits on VL2

Similar to VL1, VL2 is driven by the user in order to locate the DMS in a more convenient position on the 3D object. Also in this case, VL2 is used when the 3D model remains fixed to the ground allowing the movement along the 'Y' axis.

7.1.3 Limits on OR1 and OR2

The OR1 and OR2 sliders that control their rotation are driven by the user when the DMS is linked to the ground through a revolute joint on slot constraint (second interaction modality described in Section 7). In other words, the DMS is

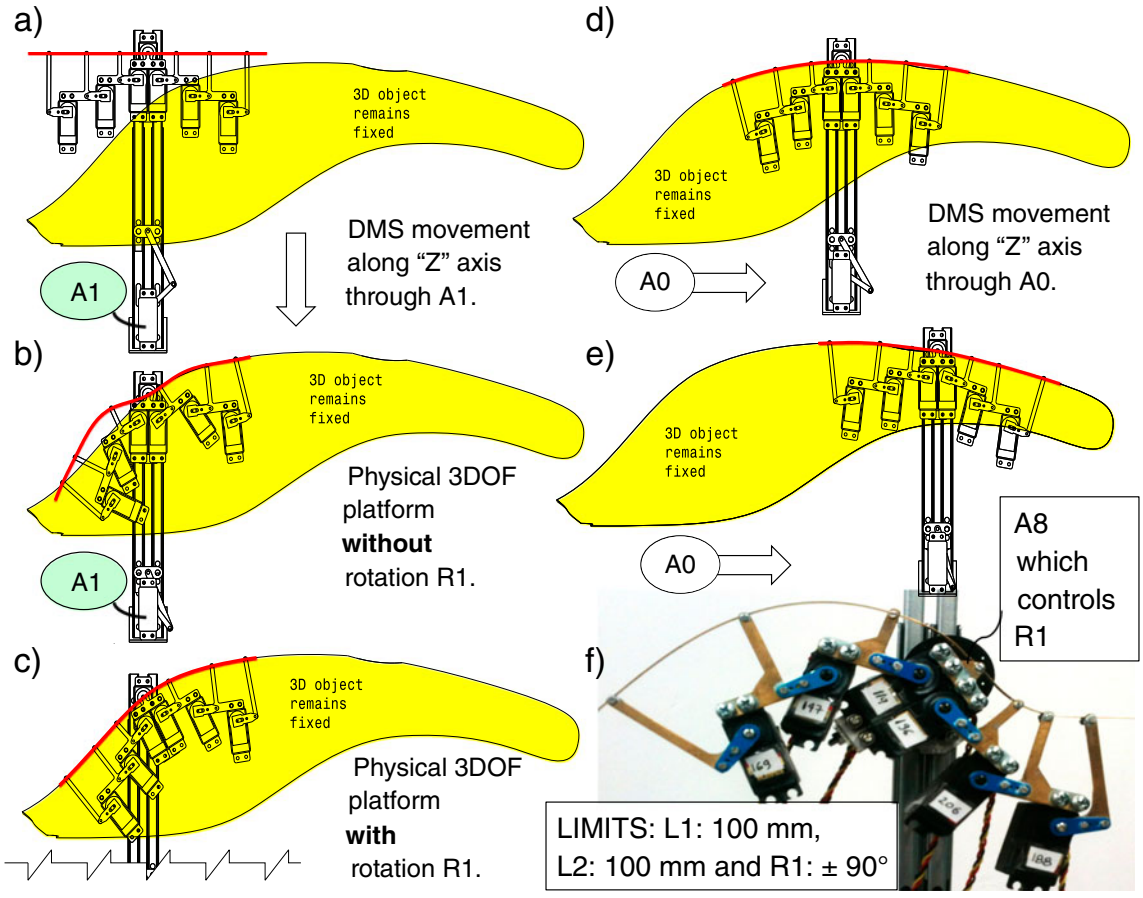

Figure 10. Limits on L1, L2 and R1.

able to move along the 'Z' axis depending on the position of interpolation point 1 (IP1). In this case, the user is able to rotate the 3D model around the 'Z' axis from +180 degrees to −180 degrees according to his needs. Figures 13-a and 13-b show the 3D object rotation through the OR1 slider. In this instant of the simulation we are also tracking the path produced by the interpolation points represented by the orange trajectories.

Figures 13-c and 13-d show the 2D cross-section rendering process performed by the DMS at different time and rotation values. The graphic displays the trajectory reached by interpolation point 4 (IP4) while the 3D object rotates.

7.1.4 Limits on OV1 and OV2

The OV1 and OV2 sliders are driven by the user in the same way as the VL1 and VL2, which move the DMS. Instead of moving the DMS, the user moves the 3D object. Obviously, in this case, the user is working with the second interaction modality, i.e. when the DMS is linked to the ground through a revolute joint on slot constraint.

8. Validation of the accuracy of the DMS

This section presents the validation of the mechatronic device, whose aim is to give rigorous, valid and practical conclusions about the accuracy of the device. In this research we have been interested in two main issues. The first was to evaluate the mechatronic device in terms of accuracy while representing a 2D cross-section; the second was to provide guidelines for the design of future similar devices, on the basis of the evaluation results.

Figure 14 shows the experimental setup used for the evaluation. Three different 2D cross-sections laying on a target object (a vacuum cleaner) have been rendered and measured in order to know the accuracy error in terms of millimetres. Figure 14-a shows the location of the three target curves, one on the left, one in the middle and one on the right hand side of the object. Figure 14-b shows the device while reaching the target curve A, and the user's hand while exploring the real vacuum cleaner. Figure 14-c shows the visual-Nastran interface and the device while reaching the target curve B, and Figure 14-d shows a visual comparison of the real vacuum cleaner and the device while reaching the target curve C.

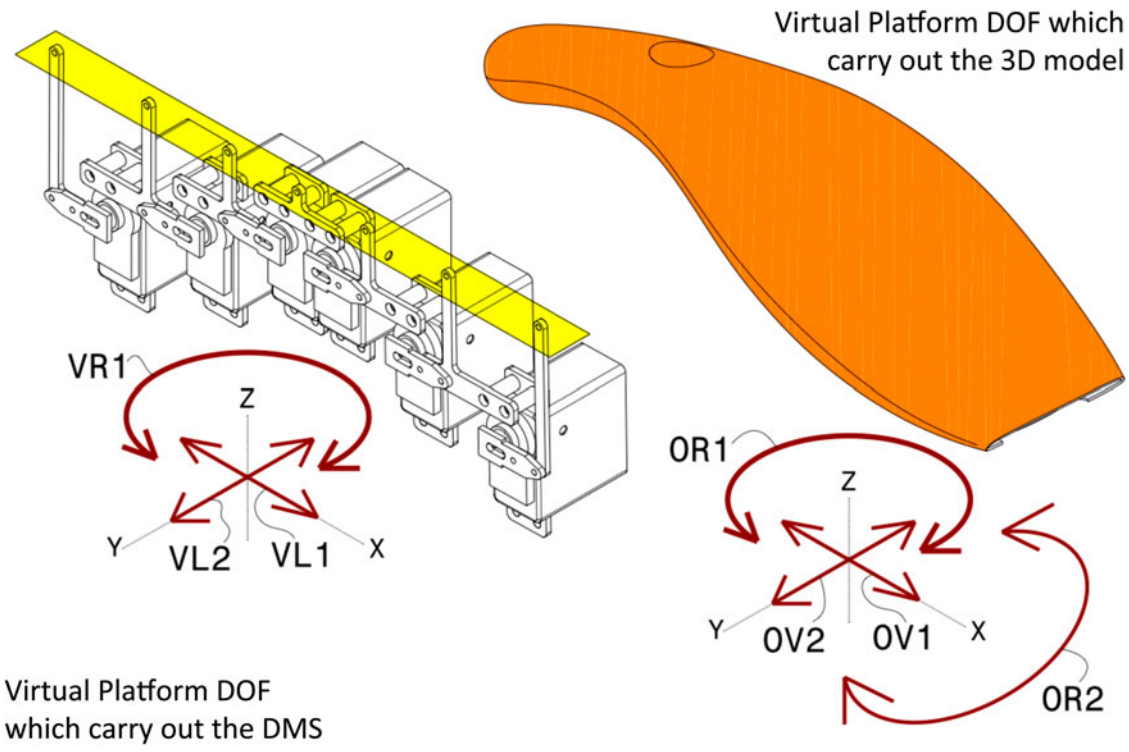

Figure 11. Virtual platforms.

In order to determine the accuracy of the desktop strip we have compared the real strip and the virtual 2D cross-section curves. A set of measurements has been performed using the Konica Minolta 3D scanner (Minolta 2012) device. This scanner has an accuracy of 50 μm enabling 3D measurements. The data have been exported in STL file format, and used to compare those with the CAD surfaces. Therefore, we have been able to measure the error in the physical strip spline.

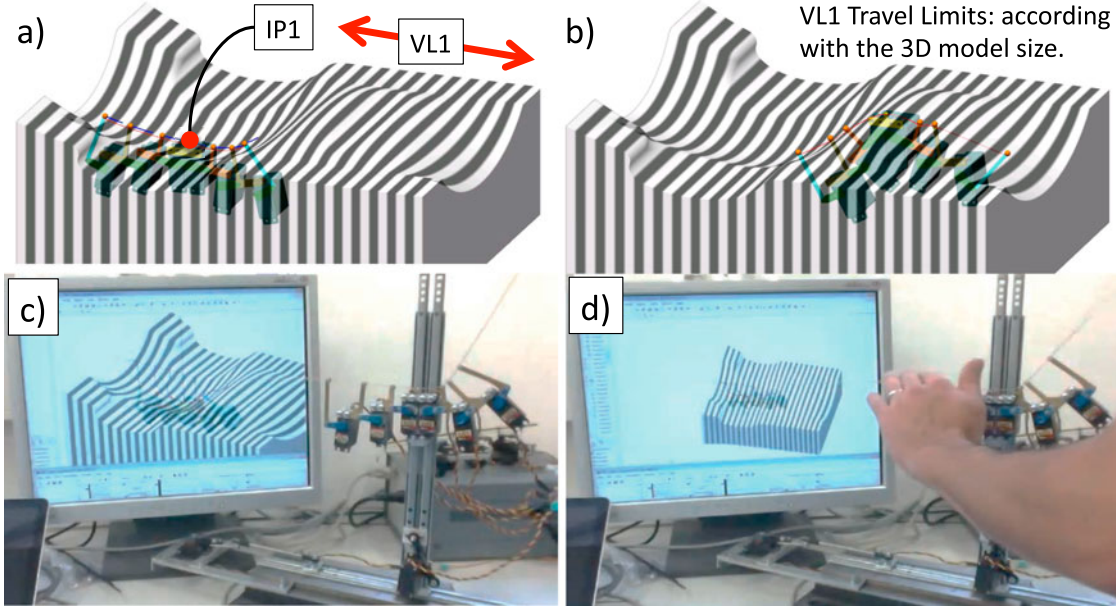

Figure 12. Limits on VL1.

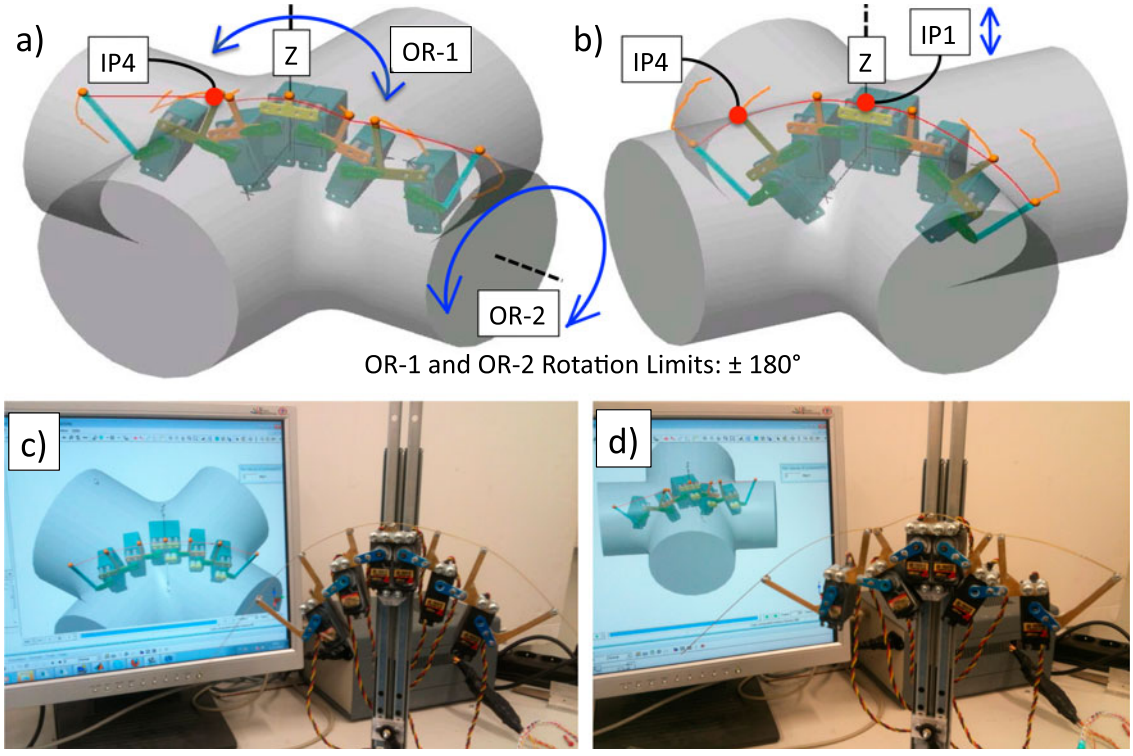

Figure 13. Rotation limits on OR1.

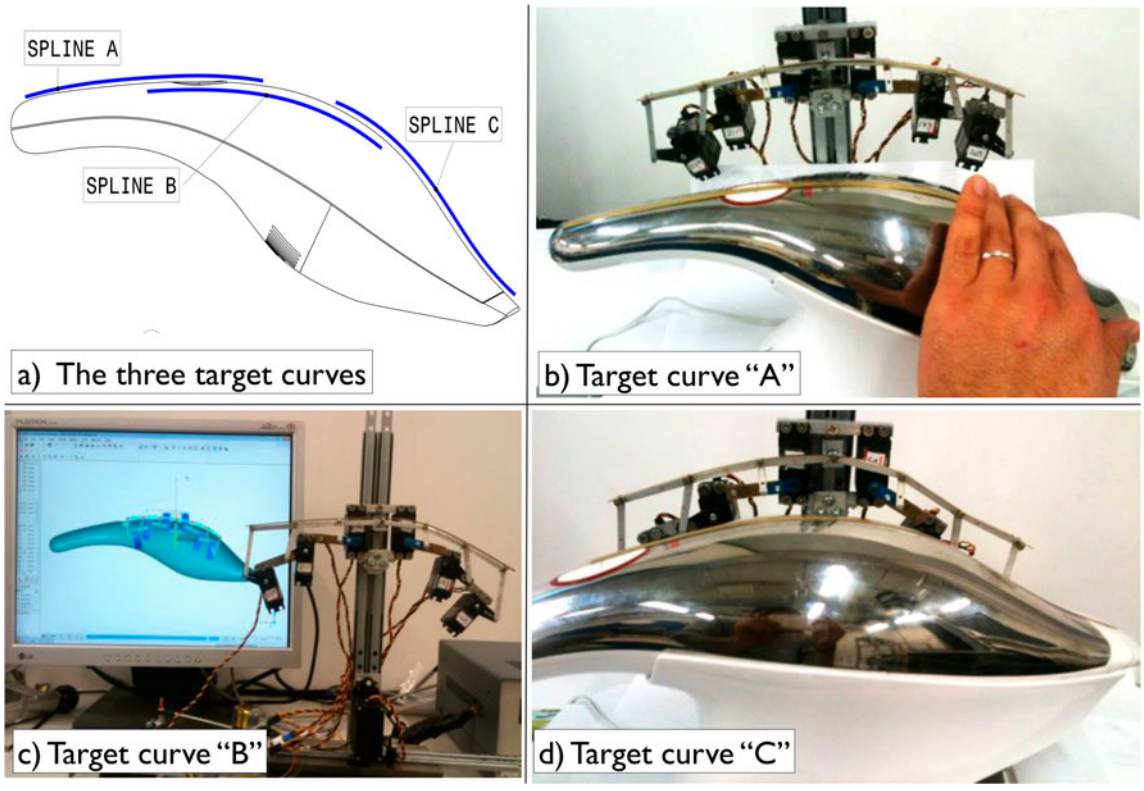

Figure 14. Experimental set-up.

8.1 Porcupine curvature analysis

A porcupine curvature analysis has been performed by considering as geometry references both convex and concave shapes. The porcupine plot is a visual curvature analysis technique for curves and surfaces, which places visual 'quills' at points along a curve. The Frenet frame of the curve determines the direction that the quill displays at that point on the curve, while the relative length of the quill reflects the curvature and/or the radius at that point. The greater the curvature of the curve at the quill point, the longer the length of the quill. In Figure 15 the curvature is illustrated by a solid grey line. Note that in this example if the porcupine quill is drawn on top of the curve shape, this denotes a negative curvature value, i.e. a convex shape, whereas a porcupine quill drawn underneath the curve shape denotes a positive curvature value, i.e. a concave shape.

For a given curve C, the curvature at point q has a magnitude equal to the reciprocal of the radius of the osculating circle, i.e. the widest circle that shares a common tangent to the curve at the contact point. For a 2D curve given explicitly as C = f(q) the curvature is given by Equation (3):

$$K = \frac{\frac{d^2c}{dq^2}}{\left(1 + \left(\frac{dc}{dq}\right)^2\right)^{\frac{3}{2}}} \tag{3}$$

Typically, in CAD tools the orientation of quills representing the curvature may be reversed, i.e. positive curvature quills are drawn on the top instead of on the bottom of the curve, and negative curvature quills are drawn underneath instead of on top.

The porcupine curvature analysis also offers the possibility to display the curvature radius instead of the curvature of the shape. We decided to use the curvature radius for the analysis presented in this section. The porcupine analysis has been performed using a parameter of density equal to 30. With this parameter, the shape curve has been segmented in various equally spaced segments. The 30 value in the density parameter is particularly useful when the geometry is too dense to be read but the resulting curve may not be smooth enough for the analysis needs. Figure 16-a shows the position of the Target Curve 'A', the theoretical and the physical strip curvature radius and the positional error.

The positional error is the distance between the theoretical spline and the physical one. In this case, the maximum error value is reported at interpolation point 6 (IP6), which is 1.4 mm. However, the average error value along the total trajectory of the spline is only 0.7 mm.

The same analysis is performed for the Target curve 'B' as can be seen in Figure 16-b, in which the curve position (theoretical and physical), the curvature radius and the positional error is also reported. In this case, the highest error value is located at interpolation point 7 (IP7) which is 2.9 mm with an average value along its length of about 1.4 mm. Finally, Figure 16-c shows the Target curve 'C' (theoretical and physical), the curvature radius and the positional error. In this case, the highest error is reported at interpolation point 1 (IP1) which is 2.9 mm. The average error while reaching this curve is 1.3 mm. The positional errors are probably occurring due to manufacturing and assembly tolerances. However the rendering physical curvature process follows the same trajectory as the target curves.

9. Conclusion

In this paper we have presented a novel Desktop Mechatronic System (DMS) based on the Minimal Energy Curve (MEC) spline approach. This mechatronic device allows a continuous and smooth, free hand contact interaction with a developable real strip actuated by a servo-controlled mechanism, which is controlled by seven interpolation points. Additionally, we have presented a successful methodology for physically rendering a 2D cross section of a virtual object through the DMS, whose aim is to allow industrial designers to explore, with the sense of touch, the surfaces of virtual objects. We have performed some preliminary tests in order to prove the concept and understand the improvements in the precision and quality of

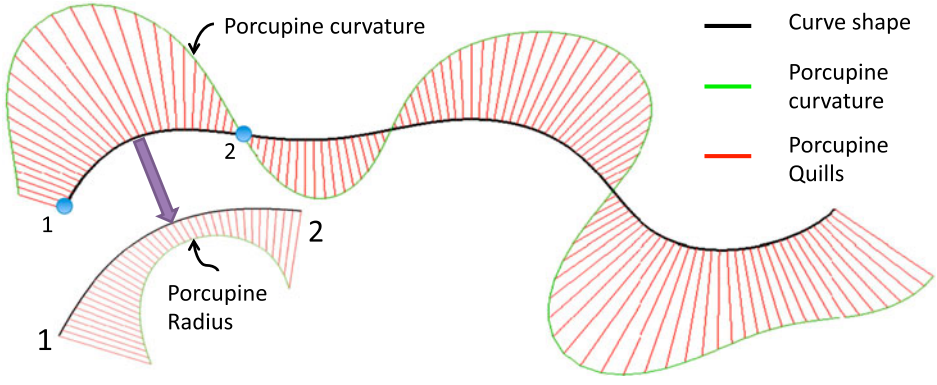

Figure 15. Curve shape with curvature and radius illustrated using a porcupine display.

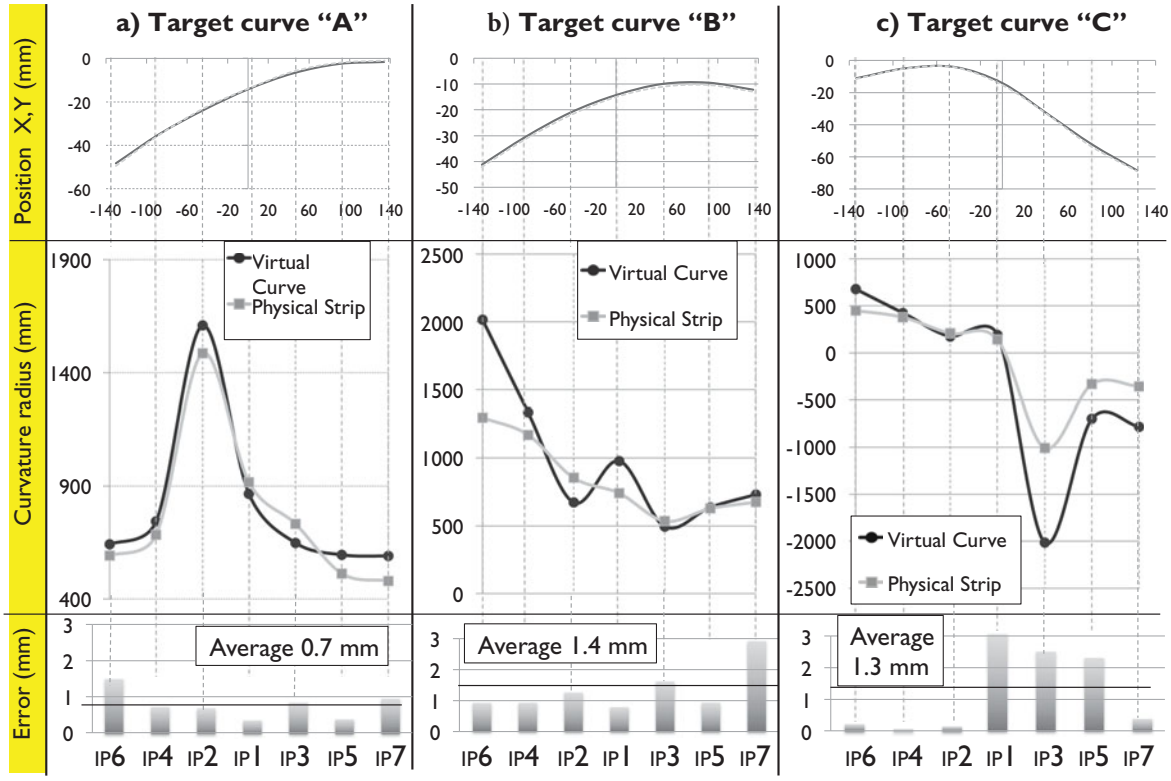

Figure 16. Vacuum cleaner 2D cross-sections.

the representation of an aesthetic surface offered by the DMS. The test results are good for what concerns the quality of the rendering of the surface, and the interaction modality proposed. Future research activity includes the integration of the DMS with a 3D visual rendering system, based on an augmented reality approach.

References

Anderl, R., Klug, L., and Mecke, K., 2006. Advanced prototyping with parametric prototypes. *In: Digital Enterprise Technology- Perspectives and Future Challenges (DET'06)*. Setubal: Springer, 503–510.

Bordegoni, M., *et al*., 2009a. Geodesic haptic device for surface rendering. *In:* M. Hirose, *et al.*, eds. *Joint virtual reality conference of EGVE – ICAT – EuroVR (2009)*. France: Eurographics.

Bordegoni, M., *et al*., 2009b. A linear haptic interface for the evaluation of shapes. *In: ASME 2009 International Design Engineering Technical Conferences (IDETC) and Computers and Information in Engineering Conference (CIE)*, 30 August, 2009, San Diego, CA, ASME.

Bordegoni, M., *et al*., 2010. Haptic and sound interface for shape rendering. *Presence: Teleoperators and Virtual Environments*, 19 (4), 341–363.

Bordegoni, M., *et al*., 2011. Geodesic spline interface for haptic curve rendering. *IEEE Transactions on Haptics*, 4 (2), 111–121.

Broek, J., Kooijman, A., and Rademacher, H., 2004. Exploration of flexible blade curvature for free form thick layered object manufacturing. *In: Proceedings of the TMCE 2004*, April 13–17, 2004, Lausanne, Switzerland.

Cao, B.W., *et al*., 2009. CAD/CAE integration frame-work with layered software architecture. *In: Proceedings of the 11th IEEE International Conference on Computer-Aided Design and Computer Graphics*, Huangshan, China, 410–415.

Covarrubias, M., Bordegoni, M., and Cugini, U., 2013. Continuous surface rendering, passing from CAD to physical representation. *International Journal of Advanced Robotic Systems* [online]. 10 Sahin Yildirim, Selcuk Erkaya, ed. ISBN: 1729-8806, InTech, DOI:10.5772/56536. [Accessed 25 Jun 2013].

Dostmohamed, H. and Hayward, V., 2005. Trajectory of contact region on the fingerpad gives the illusion of haptic shape. *Experimental Brain Research*, 164 (3), 387–394.

Frisoli, A., *et al*., 2008. A fingertip haptic display for improving curvature discrimination. *Presence: Teleoperators and Virtual Environments*, 17 (6), 550–561.

Giberti, H., Cinquemani, S., and Ambrosetti, S., in press. 5R 2dof parallel kinematic manipulator – A multidisciplinary test case in mechatronics. *Mechatronics*.

Gibson, I., Gao, Z., and Campbell, R., 2005. A comparative study of virtual prototyping and physical prototyping. *International Journal of Manufacturing Technology and Management*, 4 (6), 503–522.

Gonenc, B. and Gurocak, H., 2012. Virtual needle insertion with haptic feedback using a hybrid actuator with DC servomotor and MR-brake with Hall-effect sensor. *Mechatronics*, 22 (8), 1161–1176.

Hitec, 2012. Hitec Servo-Actuators Inc. [online]. Available from http://www.hitecrcd.com [Accessed 19 Apr 2013].

Horváth, I., *et al*., 1998a. Tool profile and tool path calculation for free-form thick-layered fabrication. *Computer-Aided Design*, 30 (14), 1097–1110.

Horváth, I., Vergeest, J.S., and Juhász, I., 1998b. Finding the shape of a flexible blade for free-form layered manufacturing of plastic foam objects. *In: Proc. of the ASME 1998 International Design Engineering Technical Conferences*, Atlanta, Georgia, USA, September 13–16, 1998.

Kallay, M., 1987. Method to approximate the space curve of least energy and prescribed length. *Computer-Aided Design*, 19 (2), 73–76.

Lammertse, P., Frederiksen, E., and Ruiter, B., 2002. The HapticMaster, a new high-performance haptic interface. *In: Proceedings of Eurohaptics 2002*, Edinburgh, UK.

Liu, B., Campbell, R.I., and Pei, E., 2013. Real-time integration of prototypes in the product development process. *Assembly Automation*, 33 (1), 22–28.

Menelas, B., *et al*., 2008. A survey on haptic interaction techniques in the exploration of large and scientific data sets. *Proceedings of Virtual Reality International Conference (2008)*, Laval, France.

Minolta, K., 2012. Konica Minolta Sensing Americas Inc. [online]. Available from: http://sensing.konicaminolta.us/applications/3d-scanners [Accessed 19 Apr 2013].

Pont, S.C., Kappers, A.M., and Koenderink, J.J., 1997. Haptic curvature discrimination at several regions of the hand. *Perception & Psychophysics*, 59 (8), 1225–1240.

Provancher, W.R., *et al*., 2005. Contact location display for haptic perception of curvature and object motion. *International Journal of Robotics Research*, 24 (9), 691–702.

Sanders, A.F. and Kappers, A.M., 2009. A kinematic cue for active haptic shape perception. *Brain Research*, 1267, 25–36.

Senkal, D. and Gurocak, H., 2011. Haptic joystick with hybrid actuator using air muscles and spherical MR-brake. *Mechatronics*, 21 (6), 951–960.